Tracing charge transfer states in polymer

Manca, Marianna; Piliego, Claudia; Wang, Ergang; Andersson, Mats R.; Mura, Andrea; Loi, Maria A.

Published in:
Journal of Materials Chemistry A

DOI:
10.1039/c3ta11005b

Publication date:
2013

Journal of Materials Chemistry A

Materials for energy and sustainability

www.rsc.org/MaterialsA

Volume 1 | Number 25 | 7 July 2013 | Pages 7279–7534

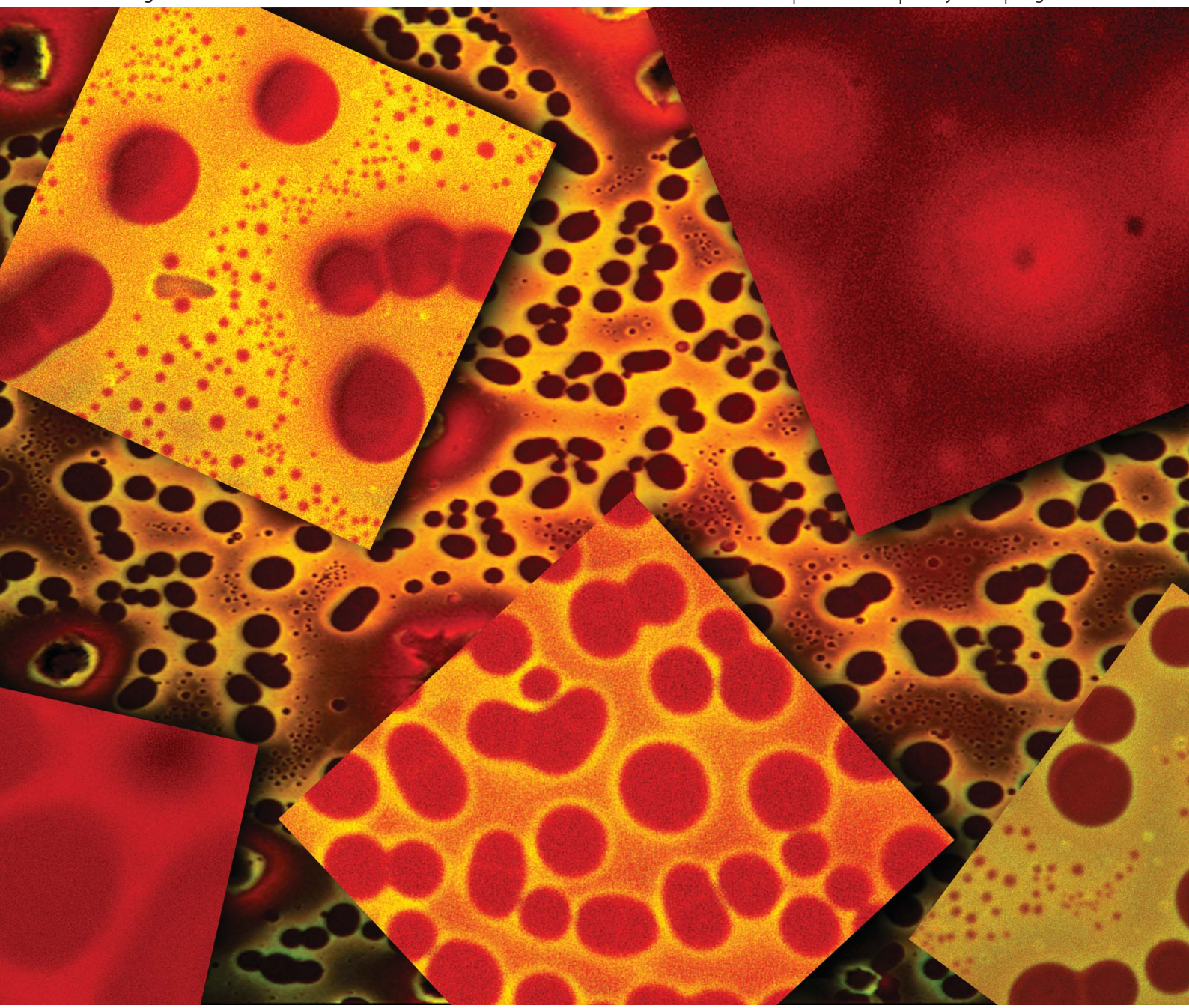

ISSN 2050-7488

RSC Publishing

PAPER

Maria A. Loi *et al.*

Tracing charge transfer states in polymer:fullerene bulk-heterojunctions

2050-7488(2013)1:25;1-W

Journal of Materials Chemistry A

RSC Publishing

PAPER

View Article Online
View Journal | View Issue

Tracing charge transfer states in polymer:fullerene bulk-heterojunctions

Cite this: *J. Mater. Chem. A*, 2013, **1**, 7321

Marianna Manca,[a] Claudia Piliego,[a] Ergang Wang,[b] Mats R. Andersson,[b] Andrea Mura[ac] and Maria A. Loi*[a]

Received 10th March 2013
Accepted 25th April 2013

DOI: 10.1039/c3ta11005b

www.rsc.org/MaterialsA

Charge transfer state emission in organic bulk-heterojunctions has been demonstrated to be an important loss mechanism for this reason a better understanding of the nature and origin of the charge transfer state is fundamental for the improvement of organic solar cells. Here, the relationship between photophysical and morphological features of a prototypical organic bulk-heterojunction is investigated in blends with different donor–acceptor ratios. By correlating imaging with photoluminescence spectra measured in different areas of the blends, the charge transfer state emission is unambiguously assigned to microscopical regions in which the intermixing of the two organic semiconductors is higher.

1 Introduction

In recent years organic bulk-heterojunction (BHJ) solar cells[1,2] have received increasing attention in the scientific community due to their potential as ultra-low-cost photovoltaic technology.[3] Due to the latest progress, the result of a large international multidisciplinary effort, the maximum efficiency reported for organic solar cells (>10%) is approaching the performance of devices based on amorphous silicon.[4]

Nowadays, fundamental research on organic solar cells focuses on understanding the factors that affect their performance and the strategies to improve it. Among the most important topics are: the tuning of the energy level offset between the components of the active layer;[5,6] the investigation of the charge generation mechanism;[7,8] the improvement of the charge transport properties of the BHJ;[9] and ultimately, the efforts to limit the recombination losses.[10]

Despite the fundamental importance of the charge generation process for the optimization of organic solar cells, this aspect of their functioning is still not fully understood and the debate is still open. In particular, whether the charge separation is a direct process mediated by a hot excited state,[11] or whether it is an ultra-fast electron transfer of thermalized excitations, is under discussion.[12,13]

Recently, the formation of *charge transfer states* (CTSs) has been observed in several bulk-heterojunctions, an overview is given in ref. 14 and references therein. In the CTS, the exciton is weakly bound by Coulombic force, with the hole and the electron localized in the donor and acceptor material, respectively.[15] CTS recombination has been demonstrated as detrimental to the overall efficiency of the device.[16,17] Therefore, a better understanding of the physics of the CTS in polymer:fullerene blends is crucial for the improvement of organic solar cells.[14,18]

From all previous studies it appears that the donor:acceptor interfacial area, the phase separation of the materials and their domain size play a crucial role in the formation of the CTS.[8,19] Therefore, identification of the position of the CTS recombination in the BHJ will allow some of the relevant properties of this state, which have an impact on the charge generation and recombination in solar cells, to be addressed. Moreover, it will provide important strategies for the suppression of CTS in BHJ solar cells.

In the most efficient bulk-heterojunction solar cell the donor and acceptor molecules form a bi-continuous composite with a maximum interfacial area for exciton dissociation, and an average domain size comparable with the exciton diffusion length (5–10 nm).[20] The extreme length scales that characterize the BHJ under the optimized conditions make it impossible to correlate specific morphological features of the film with the optical properties of different regions. The only possible strategy to overcome this problem is to use a coarser morphology than the one used in solar cells. Recently, Grancini and co-workers adopted this approach to correlate morphology with CTS dynamics in P3HT:fullerene blends by using ultrafast confocal pump–probe.[21] In their work a long-lived signal assigned to the CTS was observed and localized at the interfacial regions between the phases of the two materials.

The aim of the present work is to understand where the CTS optical recombination is localized in a prototypical BHJ, such as the one composed of poly((2,7-(9,9-(di-*n*-octyl)fluorene)-*alt*-5,5-(4′,7′-di-thienyl-2′,1′,3′-benzothiadiazole))) (APFO3) and

[a]*Zernike Institute for Advanced Materials, University of Groningen, Nijenborgh 4, Groningen, 9747 AG, The Netherlands. E-mail: M.A.Loi@rug.nl*

[b]*Department of Chemical and Biological Engineering/Polymer Technology, Chalmers University of Technology, SE-412 96 Göteborg, Sweden*

[c]*Dipartimento di Fisica, Università degli Studi di Cagliari, I-09042 Monserrato CA, Italy*

[6,6]-phenyl-C61-butyric acid methyl ester (PCBM). Our approach to the problem differs from the one adopted previously;[21] combining confocal laser scanning microscopy (CLSM) and spatially resolved photoluminescence (PL) spectroscopy, we address directly the problem of the CTS recombination allowing a more straightforward interpretation of the results with respect to the problem of the recombination losses in devices. With our technique we reach a spatial resolution below 300 nm and by measuring the PL signal we obtain higher detection sensitivity with lower excitation power with respect to the one reachable with pump–probe.

By analysing blends with different donor–acceptor ratios, we measured the stronger CTS emission from regions of the blend in which the intermixing of the two materials is higher. This result provides a clear strategy to modify the morphology of the BHJ, to suppress the CTS, and consequently to reduce recombination losses in solar cells.

2 Results and discussion

The blend of APFO3 and PCBM is a reference system for the study of CTS recombination.[19,22–25] Here the CTSs manifest themselves with a featureless emission peak at lower energy with respect to the polymer emission, which cannot be related either to the emission of the polymer or to that of the fullerene molecules. Furthermore, it was observed that by increasing the PCBM percentage in the blend, the emission of the CTS undergoes a strong redshift due to the variation in the average dielectric constant of the medium.[19,22]

In order to spatially resolve the regions of the blend with different compositions by CLSM measurements, we prepared samples with a coarsened morphology with respect to the one that gives the solar cells with the best power conversion efficiencies.[26,27] Two sets of samples (66% PCBM (1 : 2) and 80% PCBM (1 : 4) blends) using drop casting from toluene solutions were prepared.

In Fig. 1 the normalized photoluminescence (PL) spectra of the APFO3 and PCBM neat films and APFO3:PCBM 1 : 2 and 1 : 4 blends are reported. The copolymer emission shows the main emission peak at ~680 nm, PCBM has a main peak at ~730 nm and a weaker shoulder at ~810 nm. The PL of the 1 : 4 blend shows the features of both the neat copolymer (~680 nm) and the fullerene derivative (~730 nm with a shoulder at ~810 nm). The presence of the emission features of both components of the blend, conversely to what is generally recorded in solar cell active layers, is due to the phase segregation induced by the preparation of the films by drop-casting from toluene.

Together with the characteristic spectral features of the pristine materials, the 1 : 2 blend shows a new peak at ~800 nm with similar intensity to the 730 nm emission peak, which cannot be associated with any of the pristine material emissions. This new feature has been attributed to the CTS emission in previous studies on the same blend.[19,22]

The fact that the CTS emission can be detected in the APFO3:PCBM 1 : 2 blend and not in the 1 : 4 blend suggests that the formation of the CTS is strongly affected by the relative concentration of the components and most importantly by the resulting morphology. In order to get deeper insights into the role of the blend morphology and to reveal the location of the CTS emission in the blend film, we performed CLSM measurements on the two different blends.

In Fig. 2a and b the confocal photoluminescence images of the APFO3:PCBM 1 : 2 and 1 : 4 blends are reported. The photoluminescence signal in the micrographs is represented with false colours, the yellow corresponds to the signal collected at 515 ± 20 nm, and the red corresponds to the emission at wavelengths longer than 650 nm. The spatial resolution of the images is estimated to be <250 nm. Both blends show a strong phase separation, characterized by three different main regions:

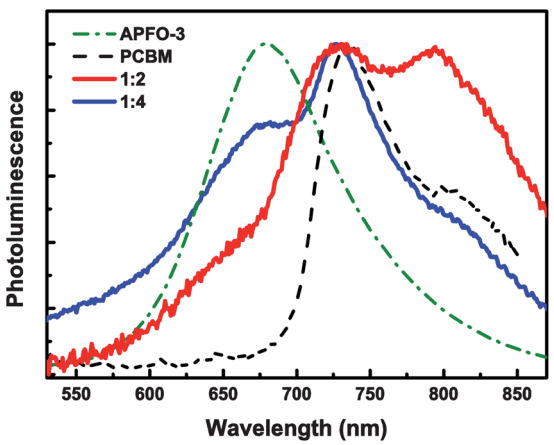

Fig. 1 Photoluminescence spectra of thin films of APFO3, PCBM and APFO3/PCBM blends (1 : 2 and 1 : 4). The spectra are normalized to the maximum intensity.

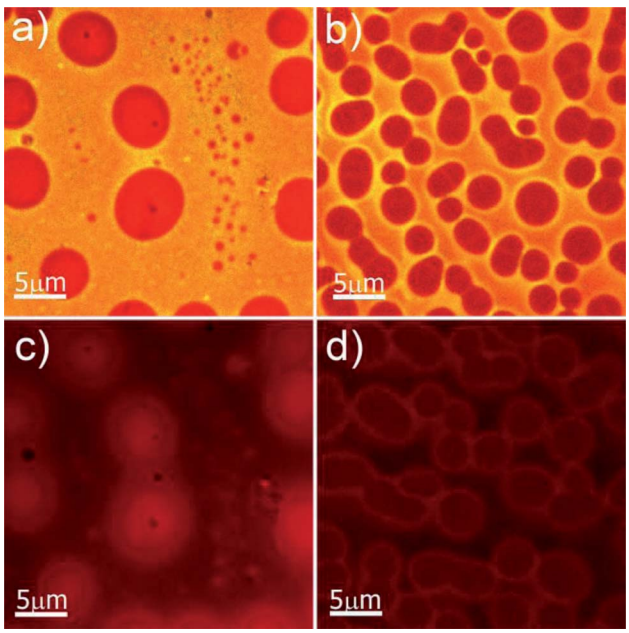

Fig. 2 CLSM images (30 μm × 30 μm) of APFO3/PCBM blends: 1 : 2 and 1 : 4 ((a and b), respectively). CLSM images recorded by using a long pass filter (780 nm) 1 : 2 blend (c) and a 1 : 4 blend (d) and exciting the samples simultaneously at 488 nm and 543 nm.

the circular domains (red colour in the micrographs), the region between the circular domains (yellow-orange colour in the micrograph) and the interfacial areas.

The dark domains are PCBM rich regions and the areas in between are polymer rich phases as indicated by the higher energy spectral components of the images. Comparing the two images (Fig. 2a and b), the APFO3:PCBM 1 : 2 blend shows a weaker phase separation with respect to the 1 : 4 blend; in the polymer rich phases of the 1 : 2 blend it is still possible to recognize small PCBM domains on the sub-500 nm length-scale.

Fig. 2c and d show the CLSM micrographs of APFO3:PCBM 1 : 2 and 1 : 4 blends, respectively, recorded by using an optical long-pass filter in front of the photomultiplier tube (PMT) array to detect the sample photoluminescence signal above 780 nm. Since the photoluminescence emission above 780 nm is mostly due to PCBM and to the CTS, we can estimate the intermixing of the two components in the blend and the presence of the CTS. While the 1 : 4 blend shows a strong photoluminescence contrast between the polymer and the PCBM rich regions, the 1 : 2 blend exhibits a diffuse emission in the polymer rich phase indicating the presence of PCBM and/or CTS emission also in these areas. In both blends, the emission at wavelength higher than 780 nm is stronger in the interfacial areas, which suggests a more pronounced morphology in this region or the presence of the low-energy emitting CTS, as proposed by Grancini *et al.*[21]

From the spatially integrated PL results reported in Fig. 1 and from the micrographs reported in Fig. 2, we infer that in order to have a good CTS emission signal a certain degree of intermixing between the two components of the blend is necessary. To confirm this hypothesis and to localize the CTS emission, we performed spatially resolved spectroscopy measurements. By recording the emission spectra point by point we are able to collect a set of data showing the spatial distribution of the PL signal. This is done by coupling the second harmonic of a Ti-Sapphire laser to the scanning head of a laser scanning confocal microscope; the photoluminescence coming from the sample is detected by three PMTs, which allows reconstructing the PL image of the sample point by point. After imaging, a specific area of the sample is excited selectively to detect the PL spectra of the region.

In Fig. 3a, the regions of different typology revealed in the imaging of the APFO:PCBM 1 : 2 film are highlighted. The spatially resolved PL spectra of these regions are shown in Fig. 3b. In this way, we are able to unambiguously determine the contributions of different blend regions to the photoluminescence emission.

The spectrum coming from the area "A" shows the typical emission of PCBM, confirming the assignment of the dark domains to PCBM rich phases. The interface spectrum, indicated by "B" in Fig. 3b, shows the spectroscopic features of both the polymer and the PCBM with a prominence of the latter. This suggests the presence of a gradient in the PCBM concentration, going toward the PCBM rich domains. The spectrum relative to the area "C", which appears homogeneously bright, corresponds to the typical APFO3 emission. While the spectrum coming from the area "D" shows the APFO3 contribution and a new emission peaked at ~800 nm, which we attribute to the CTS emission.

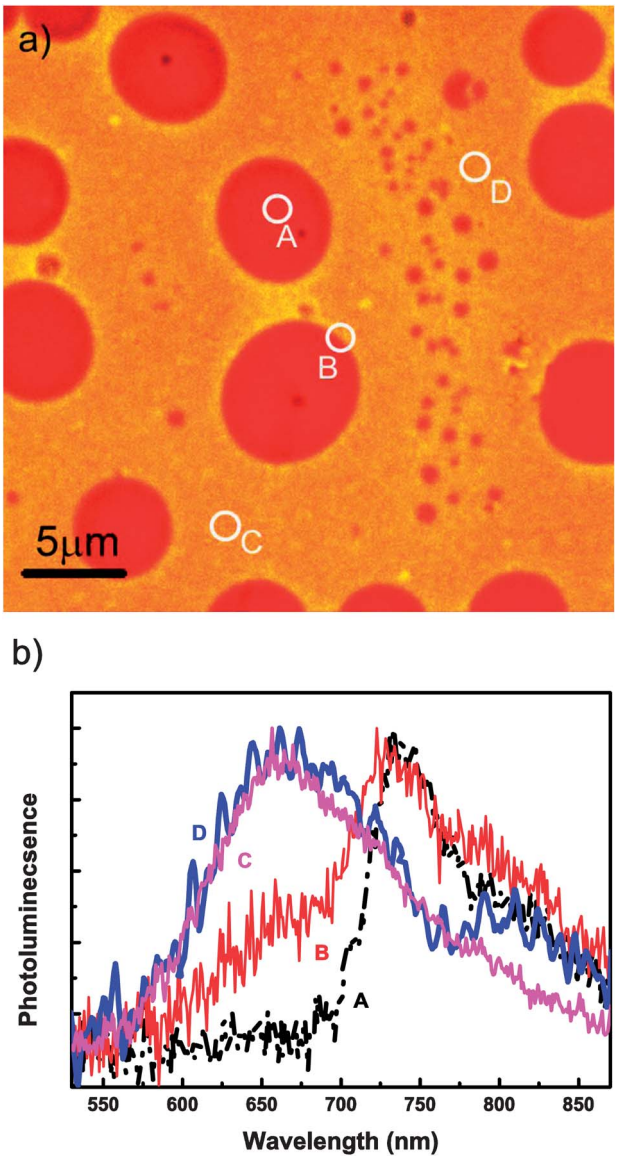

Fig. 3 (a) CLSM image of the APFO3/PCBM 1 : 2 blend and (b) PL spectra recorded in a PCBM rich region (circle A), in an interfacial region (circle B), in a polymer rich region (circle C), and in a region of high intermixing between the two materials (circle D).

It is important to notice that the CTS emission in the APFO3-PCBM blend occurs in the same spectral range of the PCBM shoulder. However, the spectrum "D" does not show any evidence of PCBM emission at 730 nm, confirming that the feature at 800 nm is determined by the CTS recombination. It has been underlined by several authors[19,22] that the wavelength of the PL emission of the CTS strongly depends on the dielectric constant of the environment, which is determined by the composition and morphology of the blend.

This results show that the CTS signal is mostly localized in areas of the sample in which the polymer and the fullerene derivative are more intimately mixed, and not in proximity of

macroscopic interfaces. This finding is in agreement with previously reported results, showing that in poly[2,6-(4,4-bis-(2-ethylhexyl)-4*H*-cyclopenta[2,1-*b*:3,4-*b*′]-dithiophene)-*alt*-4,7-(2,1,3-benzothiadiazole)] (PCPDTBT):PCBM blends the CTS emission is suppressed when processing the samples with 1,8-octanedithiol (ODT).[17] The addition of the high boiling point solvent promotes the polymer crystallization and the formation of bigger domains, preventing an excessive intermixing. Similarly, the highly crystalline poly[(4,4′-bis(2-ethylhexyl)-dithieno[3,2-*b*:2′,3′-*d*]silole)-2,6-diyl-*alt*-(4,7-bis(2-thienyl)-2,1,3-benzothiadiazole)-5,5′-diyl] (Si-PCPDTBT) was found to be not affected by the CTS recombination because of its tendency to form crystalline domains.[16,20]

3 Experimental section

Materials

APFO3 was synthesized by following the procedure reported in the literature[28] and PCBM was purchased from Solenne BV. The solutions of the pristine APFO3 and PCBM, and the blends (66% PCBM and 80% PCBM) in toluene were drop cast on clean glass substrates. The samples were kept in a nitrogen atmosphere overnight to let the solution dry slowly. This procedure allowed getting coarsened blend morphology, suitable for our microscopy study.

Measurements

Confocal laser scanning microscopy (CLSM) and spatially resolved photoluminescence (PL) measurements were performed with an experimental set up based on a Nikon Eclipse Ti microscope in backscattering configuration. The excitation source was a mode-locked Ti:sapphire femtosecond laser (Coherent) tunable in the range ~720 to 980 nm, which is characterized by pulses of ~150 fs, with a repetition frequency of ~76 MHz. By coupling the laser beam into a nonlinear LBO crystal the second harmonic (360–590 nm) can be generated. The second harmonic is coupled into the scanning head of the microscope by means of an external optical system based on a microscope objective and a single mode optical fiber.

Sample imaging is obtained by means of a set of photomultiplier tubes (PMTs), which covers a detection spectral range from ~460 to 750 nm. The spatial resolution achievable, depending on the excitation wavelength, is given by the equation:

$$d = 0.46\lambda/\mathrm{NA},$$

where λ is the excitation wavelength and NA is the numerical aperture of the microscope objective.

Spatially resolved PL spectroscopy was performed by collecting the photoluminescence signal with a monochromator coupled with a Hamamatsu Si CCD camera.

After raster scanning and imaging of the sample with an array of PMTs, which can detect the signal in three different spectral regions (515 ± 20 nm, 590 ± 20 nm and >650 nm), the laser beam is addressed in specific positions (dimensions smaller than 1 μm^2) of the sample, for each position the signal is spectrally dispersed and measured with a Si CCD camera (Image EM CCD camera from Hamamatsu).

All PL measurements are performed by exciting the sample at 380 nm using a 60 times magnification oil immersion objective with NA = 1.4. Imaging was performed by exciting at different wavelengths. All measurements have been performed in air and at room temperature.

4 Conclusions

We investigate and correlate the photophysical and morphological features of blends of APFO3 and PCBM. The integrated photoluminescence spectrum of the 66% blend shows a strong emission at ~800 nm ascribed to the CTS recombination. By correlating imaging with PL spectra measured in different areas of the 66% PCBM film, we assign unambiguously the CTS emission to microscopical regions in which the intermixing between the two materials is higher, confirming the results of previous indirect experiments on different BHJs. Finally, the combination of CLSM imaging and advanced photoluminescence measurements turned out to be a powerful tool for understanding the physics of the BHJ, when the morphological characteristics of the film can be revealed.

Acknowledgements

The work in Groningen is funded by FOM BRM project # 437155 and FOM focus group Groningen. M. A. Loi and A. Mura acknowledge NWO for the "bezoekerbeurs" financing the stay of A. M. in Groningen. E. W. acknowledges the financial support from the Swedish Research Council. We acknowledge the expert technical support of A. F. Kamp and F. van der Horst.

References

1 G. Yu, J. Gao, J. C. Hummelen, F. Wudl and A. Heeger, *Science*, 1995, **270**, 1789.
2 C. J. Brabec, N. S. Sariciftci and J. C. Hummelen, *Adv. Funct. Mater.*, 2001, **11**, 15.
3 G. Li, R. Zhu and Y. Yang, *Nat. Photonics*, 2012, **6**, 153.
4 M. A. Green, K. Emery, Y. Hishikawa, W. Warta and E. D. Dunlop, *Prog. Photovoltaics*, 2012, **20**, 606.
5 C. J. Brabec, A. Cravino, D. Meissner, N. S. Sariciftci, T. Fromherz, M. T. Rispens, L. Sanchez and J. C. Hummelen, *Adv. Funct. Mater.*, 2001, **11**, 374.
6 P. W. M. Blom, V. D. Mihailetchi, L. J. A. Koster and D. E. Markov, *Adv. Mater.*, 2007, **19**, 1551.
7 T. M. Clarke and J. R. Durrant, *Chem. Rev.*, 2010, **110**, 6736.
8 D. Jarzab, F. Cordella, J. Gao, M. Scharber, H.-J. Egelhaaf and M. A. Loi, *Adv. Energy Mater.*, 2011, **1**, 604.
9 F. Padinger, R. S. Rittberger and N. S. Sariciftci, *Adv. Funct. Mater.*, 2003, **13**, 85.
10 A. Pivrikas, N. S. Sariciftci, G. Juška and R. Österbacka, *Progr. Photovolt.: Res. Appl.*, 2007, **15**, 677.
11 G. Grancini, M. Maiuri, D. Fazzi, A. Petrozza, H.-J. Egelhaaf, D. Brida, G. Cerullo and G. Lanzani, *Nat. Mater.*, 2013, **12**, 29.

12 B. Kraabel, D. McBranch, N. S. Sariciftci, D. Moses and A. J. Heeger, *Phys. Rev. B: Condens. Matter*, 1994, **50**, 18543.
13 C. J. Brabec, G. Zerza, G. Cerullo, S. De Silvestri, S. Luzzati, J. C. Hummelen and S. Sariciftci, *Chem. Phys. Lett.*, 2001, **340**, 232.
14 C. Piliego and M. A. Loi, *J. Mater. Chem.*, 2012, **22**, 4141.
15 M. Pope and C. E. Swenberg, in *Electronic Process in Organic Crystals and Polymer*, Oxford University Press, Claredon Press, Oxford, 1998, ch. 1.
16 M. C. Scharber, M. Koppe, J. Gao, F. Cordella, M. A. Loi, P. Denk, M. Morana, H. Egelhaaf, K. Forberich, G. Dennler, R. Gaudiana, D. Waller, Z. Zhu, X. Shi and C. J. Brabec, *Adv. Mater.*, 2010, **22**, 367.
17 M. C. Scharber, C. Lungenschmied, H.-J. Egelhaaf, G. Matt, M. Bednorz, T. Fromherz, J. Gao, D. Jarzab and M. A. Loi, *Energy Environ. Sci.*, 2011, **4**, 5077.
18 K. Vandewal, K. Tvingstedt, A. Gadisa, O. Inganas and J. V. Manca, *Nat. Mater.*, 2009, **8**, 904.
19 M. A. Loi, S. Toffanin, M. Muccini, M. Forster, U. Scherf and M. C. Scharber, *Adv. Funct. Mater.*, 2007, **17**, 2111.
20 O. V. Mikhnenko, H. Azimi, M. Scharber, M. Morana, P. W. M. Blom and M. A. Loi, *Energy Environ. Sci.*, 2012, **5**, 6960.
21 G. Grancini, D. Polli, D. Fazzi, J. Cabanillas-Gonzalez, G. Cerullo and G. Lanzani, *J. Phys. Chem. Lett.*, 2011, **2**, 1099.
22 D. Veldman, O. Ipek, S. C. J. Meskers, J. Sweelssen, M. M. Koetse, S. C. Veenstra, J. M. Kroon, S. S. van Bavel, J. Loos and R. A. J. Janssen, *J. Am. Chem. Soc.*, 2008, **130**, 7721.
23 K. Tvingstedt, K. Vandewal, A. Gadisa, F. Zhang, J. Manca and O. Inganäs, *J. Am. Chem. Soc.*, 2009, **131**, 11819.
24 K. Tvingstedt, K. Vandewal, F. Zhang and O. Inganäs, *J. Phys. Chem. C*, 2010, **114**, 21824.
25 S. K. Pal, T. Kesti, M. Maiti, F. Zhang, O. Inganäs, S. Hellström, M. R. Andersson, F. Oswald, F. Langa, T. Österman, T. Pascher, A. Yartsev and V. Sundström, *J. Am. Chem. Soc.*, 2010, **132**, 12440.
26 M. Svensson, F. Zhang, S. C. Veenstra, W. J. H. Verhees, J. C. Hummelen, J. M. Kroon, O. Inganäs and M. R. Andersson, *Adv. Mater.*, 2003, **15**, 988.
27 L. H. Slooff, S. C. Veenstra, J. M. Kroon, D. J. D. Moet, J. Sweelssen and M. M. Koetse, *Appl. Phys. Lett.*, 2007, **90**, 143506.
28 O. Inganäs, M. Svensson, F. Zhang, A. Gadisa, N. K. Persson, X. Wang and M. R. Andersson, *Appl. Phys. A: Mater. Sci. Process.*, 2004, **79**, 31.